Fermilab FERMILAB-CONF-06-459-E

Results on QCD Physics from the CDF-II Experiment

C. Pagliarone*

Universitá di Cassino & INFN Pisa, Italy

(on the behalf of the CDF-II Collaboration)

Abstract

In this paper we review a selection of recent results obtained, in the area of QCD physics, from the CDF-II experiment that studies $p\bar{p}$ collisions at $\sqrt{s}$=1.96 TeV provided by the Fermilab Tevatron Collider. All results shown correspond to analysis performed using the Tevatron Run II data samples. In particular we will illustrate the progress achieved and the status of our studies on the following QCD processes: jet inclusive production, using different jet clustering algorithm, $W(\rightarrow e\nu_e)+$jets and $Z(\rightarrow e^+e^-)+$jets production, $\gamma+b-$jet production, dijet production in double pomeron exchange and finally exclusive e^+e^- and $\gamma\gamma$ production. No deviations from the Standard Model have been observed so far.

1 Introduction

The Quantum Chromo Dynamics (QCD) processes provide signals to test theoretical calculations and models and contribute major backgrounds to many other searches or measurements. Thus, their detailed understanding and modelling is of crucial importance. In particular, the current QCD physics program, at Tevatron, includes studies of jets with the goal of performing precision measurements to test and further constrain the validity of the Standard Model (SM). Jets can be defined as collimated sprays of particles originating, all in one point, from the fragmentation of a parton. The ability in reconstructing the jets allows to characterize and measure the energy of the parent partons. As jet calculations, at leading order and at higher orders, can vary the definition of a jet it is therefore important in order to compute the jet energy beyond the leading order. Jet energies are measured experimentally by adding the energy of the calorimeter cells associated to a cluster, using

*Corresponding author. E-mail: pagliarone@fnal.gov

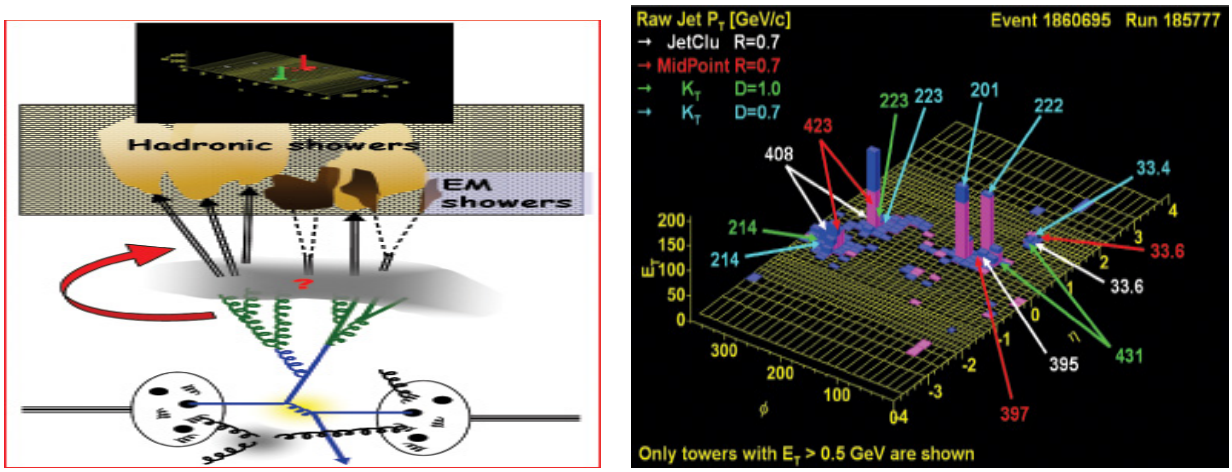

Figure 1: a) Well-defined algorithms for clustering calorimeter towers into jets is needed in order to make measurements and for comparison with theoretical predictions; b) Different Algorithms give different results.

predetermined algorithms. During Run II, CDF-II have been studying alternative methods to the fixed cone-based jet clustering algorithm, the so called JetClu [1] used during the Tevatron Run I (1992-1995). This is needed in order to avoid problems of infrared and collinear divergences due to soft partons and below/above threshold particle emission. Both MidPoint[2] and k_T[3] jet reconstruction algorithms have been used in Run II (see Fig. 1). The former is an improved version of the seed cone-based JetClu algorithm which reduces the sensitivity to infrared and collinear problems. The latter starts by finding pairs of nearby particles in the defined phase-space and then merges them together to form new pseudo-particles, continuing until a set of stable well-separated jets are found. This algorithm is infrared and collinear safe to all orders in perturbative QCD (pQCD). In addition to the energy from the primary parton, jets accrue soft contributions from the underlying event (UE) of beam remnants. These contributions become more important at smaller jet p_T [9]. During Run I and Run II, the contribution from UE energy has been studied and a modification to Pythia [4] Monte Carlo (MC) has been determined (Tune A [5]) using CDF-II data. Pythia MC with the new set of parameters describes well the jet shapes measured in Run II [6].

2 The CDF-II Detector

CDF-II is a 5000 ton multi-purpose particle physics experiment [7] dedicated to the study of proton-antiproton collisions at the Fermilab Tevatron collider. It was designed, built and operated by a team of physicists, technicians and engineers that by now spans over 44 institutions and includes, approximately, more than 500 members. The history of the experiment goes back over 20

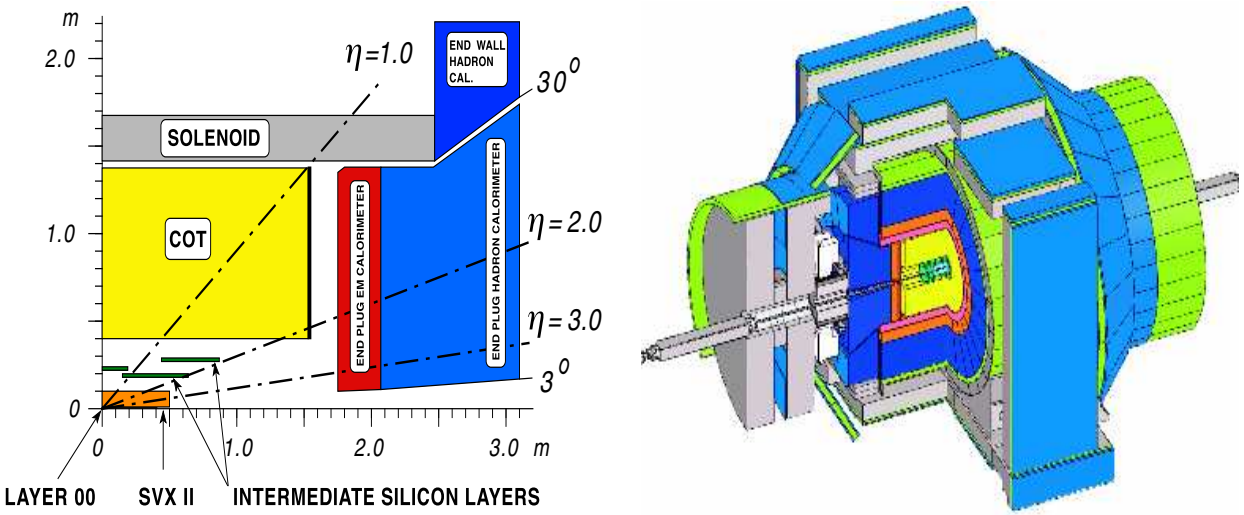

Figure 2: a) An overview of the Collider Detector at Fermilab (CDF) in its Run II configuration (CDF-II). b) A cutaway view of one quadrant of the inner portion of the CDF-II detector showing the tracking region surrounded by the solenoid and end-cap calorimeters.

years. The CDF detector has been upgraded [8] in order to be able to operate at the high radiation and high crossing rate of the Run II Tevatron environment. In addition, there have been several changes to improve the sensitivity of the detector to specific physics channels such as heavy flavor physics, Higgs boson searches and many others. Fig. 2.a shows an isometric cutaway view of the final configuration of the CDF-II detector. The central tracking volume of the CDF experiment has been replaced entirely with new detectors (see Fig. 2), the central calorimeters has not been changed. These upgrades can be summarized as follows: a new Silicon System done of 3 different tracking detector subsystems: Layer00 installed directly on the beam pipe, a new Silicon Vertex Detector (SVX II), an Intermediate Silicon Layer detector (ISL); a new central tracker the Central Outer Tracker (COT) that is an open cell drift chamber able to operate at a beam crossing time of 132 ns with a maximum drift time of $\sim$100 ns; a scintillator based Time-of-Flight detector (TOF), new Plug Calorimeters and an extended upgraded Muon system that almost doubled the coverage in the central; A new Data Acquisition System (DAQ) has also been constructed in order to operate in the shorter bunch spacing conditions.

3 QCD Results from CDF-II

3.1 Inclusive jet production: Midpoint and K_T Analysis

There are many important reason to study the inclusive jet production at Tevatron. As matter of fact it is a stringent QCD test up to $8 \div 9$ order

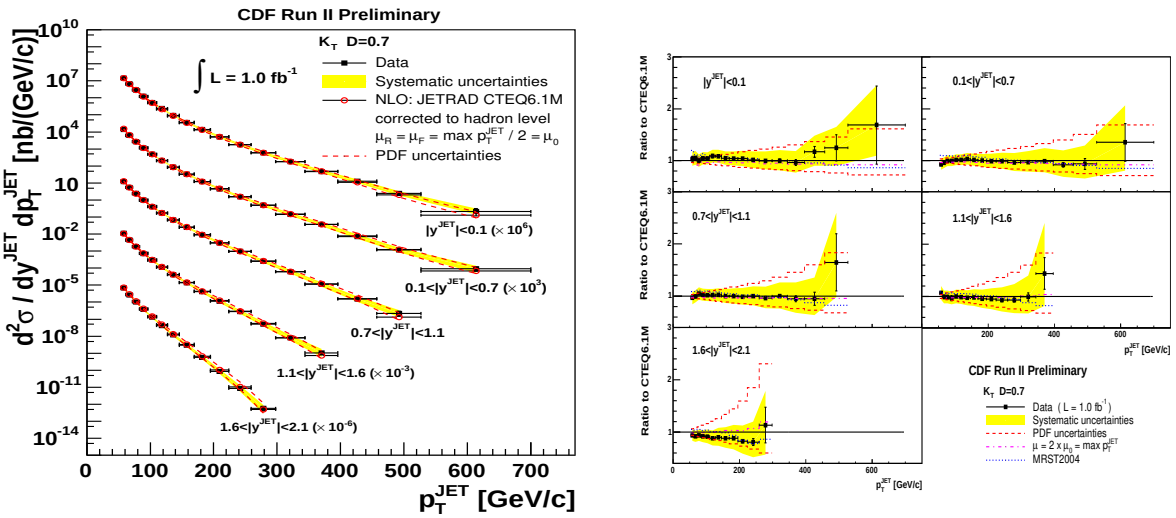

Figure 3: Jet Inclusive Cross section for jets defined using the K_T algorithm. a) Cross section in five rapidity bins (black dots) as a function of p_T^{jet} compared to NLO pQCD predictions (histogram). The shaded bands show the total systematic uncertainty on the measurement. b) Ratio of data to theory as a function of p_T^{jet}. The error bars (shaded band) show the total statistical (systematic) uncertainty on the data.

of magnitude; it is a measurement sensitive to the structure of the parton distribution functions (PDF); it helps to add constrains on gluon structure of the PDFs at high$-x$; it's a test sensitive to distances up to 10^{-19} m and it is an important tool for searching for New Phenomena. The increase in center of mass energy, from 1.80 (Run I) to 1.96 TeV (Run II), results in a larger kinematical range for measuring the jet production. The inclusive jet production cross section have been measured at CDF-II using two different jet definitions: the k_T algorithm and the MidPoint cone algorithm. The jets were selected with $p_T^{jet} \geq 54$ GeV/c in five different jet rapidity regions: $|y| < 0.1$, $0.1 < |y| < 0.7$, $0.7 < |y| < 1.1$, $1.1 < |y| < 1.6$, and $1.6 < |y| < 2.1$ [9]. The results shown in this paper are based on 1.04 fb^{-1} and are recently updated results. The experimental data are in agreement with next-to-leading order (NLO) calculations (see Fig. 3 and Fig. 4). In particular the CDF-II measurements of the inclusive jet cross section, using the k_T algorithm, show that this algorithm works well in hadron collider environment in the p_T^{jet} range studied.

3.2 W/Z boson + jets production

The production of W/Z+jets provides a good test of pQCD, in a multi-jet environment, since the presence of the W/Z ensures that the event has a high Q^2. More importantly, $W/Z+$ jets is a possible signature for many new and important processes such as the production of top pairs and single top quark production, the Higgs boson, and Supersymmetric particles. QCD production

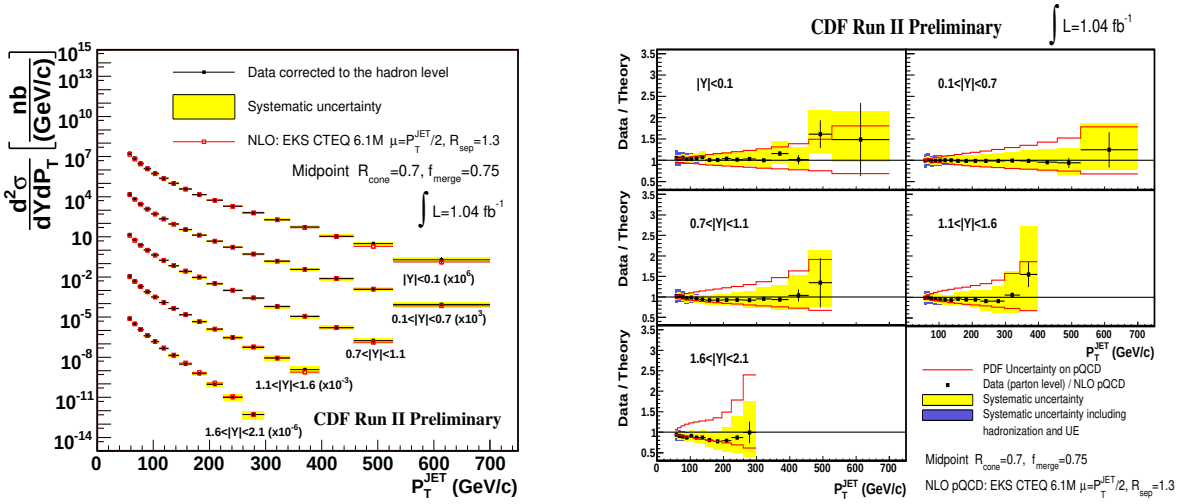

Figure 4: Jet Inclusive Cross section for jets defined using the MidPoint algorithm. a) Cross section in five rapidity bins (black dots) as a function of p_T^{jet} compared to NLO pQCD predictions (histogram). The shaded bands show the total systematic uncertainty on the measurement. b) Ratio of data to theory as a function of p_T^{jet}. The error bars (shaded band) show the total statistical (systematic) uncertainty on the data.

of W/Z+jets is a large background for many of these searches, and therefore, it is important to measure its cross section. QCD Matrix Element (ME) calculations are used to describe the hard scattering in W/Z+ jet events, and then Parton Showering Monte Carlo (PS) is used in order to simulate the soft radiation and hadronization. An overlap in phase space between $W/Z + n$ partons and $W/Z + (n + 1)$ partons can lead to double counting when combining MC samples to obtain $W/Z + n$ jets.

3.2.1 W($\rightarrow e\nu_e$)+jets production

CDF-II has measured the $W(\rightarrow e\nu_e)$+ jets cross section for W plus at least 1, 2, 3 and 4 jets, as a function of the jet transverse energy (E_T^{jet}). We also measured the $W(\rightarrow e\nu_e)$+ jets cross section for events with two or more jets, as a function of the dijet invariant mass ($M(j_1, j_2)$), and as a function of the distance in the $\eta - \phi$ plane between the leading jets ($\Delta R \equiv \sqrt{(\phi_{j_1} - \phi_{j_2})^2 + (\eta_{j_1} - \eta_{j_2})^2}$). In order to be model independent, the analysis have been performed in a restricted W kinematics phase space.
Events were selected requiring the presence of an isolated electron, in the fiducial rapidity region $|\eta(e)| < 1.1$ with $E_T^e > 20.0$ GeV, the presence of missing transverse energy ($\not\!\!E_T$) with $\not\!\!E_T > 30$ GeV [9], and finally the presence of jets having $|\eta(jet)| < 2.0$ and $E_T^{jet} > 15.0$ GeV. The reconstructed transverse W mass was required to be $M_T^W > 20.0$ GeV. Jets were reconstructed using the JetClu algorithm and corrected at hadron level; no underlying event corrections were applied. The comparison between data and theoretical calculations

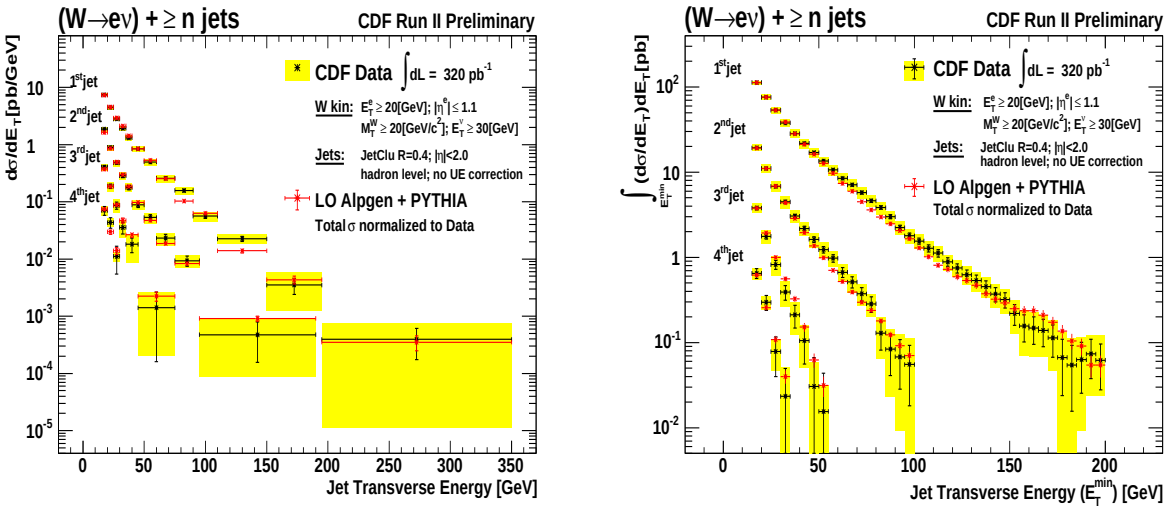

Figure 5: $W(\rightarrow e\nu_e)+$jet production. a) Differential cross-section for the leading jet in ≥ 1 jet events, second jet ≥ 2 jets events, third jet ≥ 3 and so on. b) Integrated cross sections from the previous plot. Here the bin is the minimum E_T above which the cross section is integrated.

have been performed using LO Alpgen MC plus Pythia PS.
The Monte Carlo normalized to the data show a good agreement with the theoretical predictions as shown in Fig. 5 and in Fig. 6.

3.2.2 $\mathbf{Z(\rightarrow e^+e^-)+}$jets production

Between the QCD analysis, CDF-II is also studying the $Z(\rightarrow e^+e^-)+$ jets production. As matter of fact a precise measurement of $Z(\rightarrow e^+e^-)+$jets cross section is fundamental in order to estimate the $Z(\rightarrow \nu_e\bar{\nu}_e)+$jets irreducible background. At the present we are looking for a Monte Carlo simulation that properly describes the final event topology. In Fig. 7.a we show the comparison of the jet production, as a function of the p_T^{jet}, in the data and in Pythia Tune A Monte Carlo simulation. Fig. 7.b gives the differential shape of the jets, plotted in steps of $\Delta R = 0.1$, using the calorimeter towers. Jets have been reconstructed using the MidPoint Algorithm with R = 0.7. Events have been selected requiring only one reconstructed vertex in the event. This analysis is in progress further results will come soon.

3.3 $\gamma + \mathbf{b}-$jet production

CDF-II is searching, starting from Run I, for events containing $\gamma + b$-jet. This class of analysis is interesting both for QCD studies both for searching for new phenomena, in particular, in the light stop scenario or looking for techniomega production. The search, that we present here, is based on 340 pb^{-1} of data, collected requiring the presence, in the events, of one isolated γ, in the fiducial rapidity region $|\eta(\gamma)| < 1.1$ with $E_T^\gamma > 26.0$ GeV, one b-jet

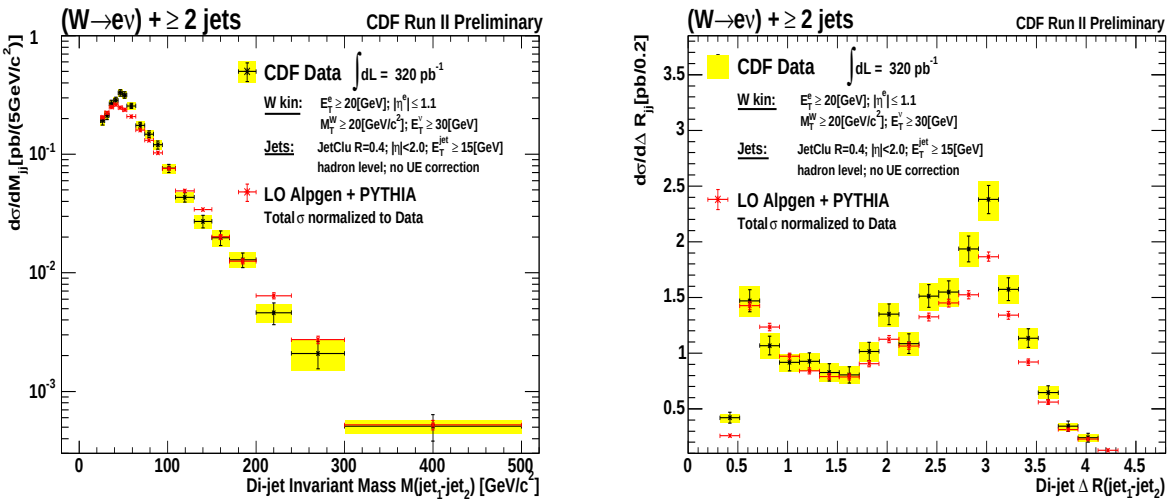

Figure 6: $W(\rightarrow e\nu_e)$+jet kinematics for $W+ \geq 2$ jets, where both jets have a minimum $E_T^{jet} > 15$ GeV. a) First-second jet invariant mass differential cross section. b) First-second jet ΔR differential cross section.

(a positively signed displaced secondary vertex) with $|\eta(b)| < 1.5$, $E_T^b > 20.0$ GeV and $\Delta R(\gamma, b) \equiv \sqrt{(\phi_\gamma - \phi_b)^2 + (\eta_\gamma - \eta_b)^2} > 0.7$.
We fit the secondary vertex mass in the data in order to determine the $b-$jet fraction. To estimate the background from fake $\gamma + b-$jet we use preshower detector information, to calculate the number of fake photons in our sample, and we multiply this by the $b-$jet fraction, previously evaluate usisng a representative background data sample. The calculated cross-section is given in the table below, where we quote the differential and inclusive cross-sections for $\gamma + b-$jet production, within the kinematical range specified in the table, given as a function of photon transverse energy (E_T^γ). The first error shown is statistical, the second is the systematic uncertainty.

CDF Run II Preliminary

Photon E_T /GeV	$\sigma(\gamma + b: \|\eta_\gamma\| < 1.1, \|\eta_b\| < 1.5, E_T b > 20)$
26-28	$2.93 \pm 0.48^{+1.04}_{-0.73}$ pb/GeV
28-31	$3.09 \pm 0.44^{+0.72}_{-0.60}$ pb/GeV
31-35	$1.46 \pm 0.23 \pm 0.33$ pb/GeV
35-43	$1.23 \pm 0.17^{+0.26}_{-0.23}$ pb/GeV
43-70	$0.23 \pm 0.03^{+0.08}_{-0.04}$ pb/GeV
> 26	$42.0 \pm 3.8^{+8.8}_{-7.0}$ pb

3.4 Dijet production in DPE

One of the most important question, in hard diffractive processes, is whether or not they obey QCD factorization. In other words, whether the pomeron has a universal, process-independent PDF. Results on diffractive Deep Inelastic Scattering (DIS) from the *ep* collider HERA show that QCD factorization

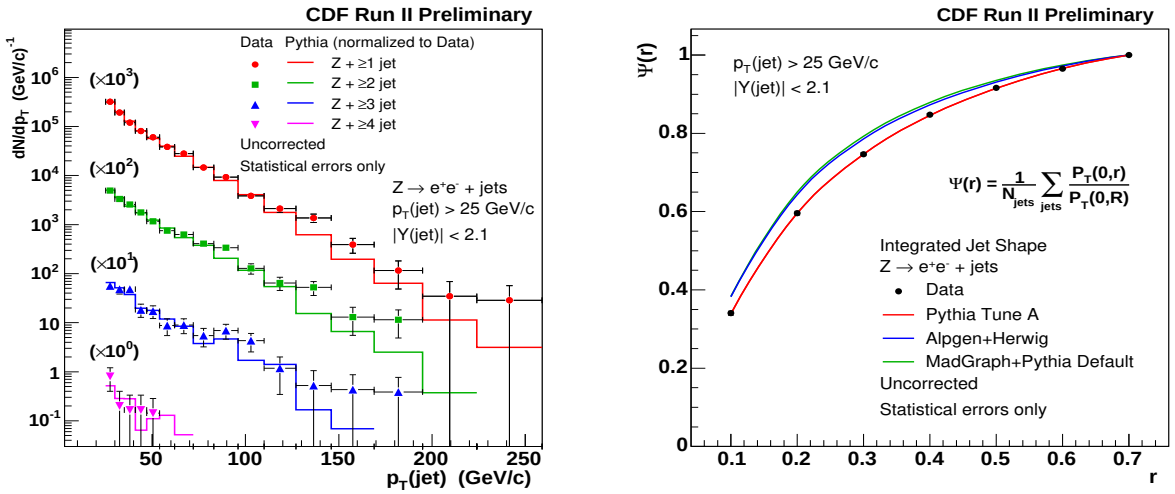

Figure 7: $Z(\rightarrow e^+e^-)$+jets production. a) Comparison of the inclusive jet production, as a function of the p_T^{jet}, in the data and in Pythia Tune A MC simulation. b) Integrated shape of the jets, plotted using the calorimeter towers. Jets are reconstructed with MidPoint algorithm with R = 0.7. The event selection requires only one reconstructed vertex in the event.

holds in DIS. Severe breakdown of QCD factorization in hard diffraction between Tevatron and HERA data have been observed. Single Diffractive (SD) process rates of dijet, W-boson, b-quark, and J/Ψ production relative to non diffractive (ND) ones, measured in Run I at CDF, are about an order of magnitude lower than expectations from PDFs determined at HERA.
The present CDF-II analysis is based on 310 pb^{-1} of data, collected with dedicated Diffractive Triggers, triggering on a leading antiproton in the Roman Pots (RP) in conjunction with a least one jet in the calorimeters. ND dijet events have been selected triggering only on jet requirements. We observe an excess of data events over the backgrounds obtained from inclusive DPE dijet Monte Carlo simulation. The observed excess is consistent with exclusive dijet Monte Carlo predictions in terms of kinematical distribution shapes. The cross sections of the observed exclusive dijet events are measured using a combination of inclusive DPE and exclusive dijet Monte Carlo simulations. The results are summarized in Fig. 8. In particular Fig. 8.a show the diffractive dijet exclusive cross section compared with the hadron level predictions, coming from the ExHuME MC simulation, and with the exclusive DPE predictions, coming from DPEMC MC simulation.

3.5 Exclusive e^+e^- and $\gamma\gamma$ production

There are SM processes in which hadrons do not dissociate in the interaction. Without hadron dissociation, there are no underlying events then we deal with very clear exclusive processes.

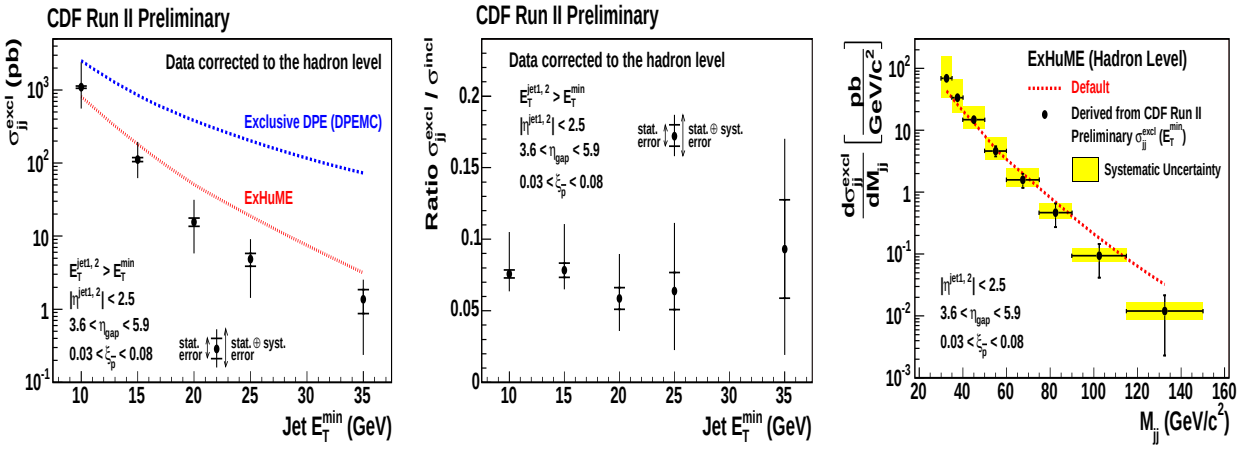

Figure 8: Dijet production in DPE: a) Comparison with hadron level predictions of ExHuME (red) and Exclusive DPE in DPEMC (blue); b) Exclusive to inclusive dijet cross section ratio vs $E_T(min)$; c) ExHuME Hadron-Level differential exclusive dijet cross section vs dijet mass.

CDF-II studied and observed two of this exclusive channels: the exclusive production of two photons via QCD (gluon exchange) and the electron pair production via QED (trough two-photon exchange).
We have observed 16 exclusive e^+e^- events with a background estimate of $2.1^{+0.7}_{-0.3}$. Each event has an e^+e^- pair ($E_T(e) > 5$ GeV, $|\eta(e)| < 2$) and nothing else observable in the CDF-II detector. The measured cross section is $\sigma = 1.6^{+0.5}_{-0.3}\,(\text{stat}) \pm 0.3\,(\text{sys})$ pb, while the predicted cross section is 1.711 ± 0.008 pb. The kinematical properties of the events are consistent with the predictions of the LPAIR Monte Carlo.
We also have evidence for 3 exclusive $\gamma\gamma$ events, with a background estimate of $0.0^{+0.2}_{-0.0}$. Each event has two photons ($E_T^\gamma > 5$ GeV, $|\eta_\gamma)| < 1$) and nothing else observable in the CDF-II detector. The measured cross section for these events is $\sigma = 0.14 \pm 0.14\,(\text{stat}) \pm 0.03\,(\text{sys})$ pb and agrees with the theoretical prediction of 0.04 pb with a factor $3 \div 5$ of theoretical uncertainty.

4 Summary

CDF-II has a broad QCD analysis program: jets, photons, bosons + jets, heavy-flavor jets, diffractive physics. The inclusive jet production have been measured with both k_T and MidPoint algorithm. Both the measurements are based on 1 fb^{-1} of data, considering 5 different rapidity regions, up to $|y| = 2.1$. A careful treatment of non perturbative effects have been taken into account. Underlying event effects have been proved to be well under control. For central jets, p_T^{jet} reach have been extended by 150 GeV/c compared to Run I. Good agreement have been found with NLO QCD calculations. Forward jet information can be used in future PDF global fits in order to better

constrain the gluon PDF at high$-x$. Good agreement, with the Theoretical expectations, have been found in all the CDF-II analysis described in this paper. We also discussed exiting observation such as: e^+e^- production via QED exchange, $\gamma\gamma$ production via QCD exchange and finally exclusive dijet production in DPE.

5 Acknowledgments

We want to thank Laszlo Jenkovszky and the Organizing Committee for their warm, kind and nice hospitality.

References

[1] F. Abe *et al.* (CDF Collaboration), Phys. Rev. D **45**, 1448 (1992).

[2] G. U. Flanagan, Ph.D. thesis, Michigan State University, 2005.

[3] S. Catani, Y. L. Dokshitzer, M. H. Seymour and B. R. Webber, Nucl. Phys. B **406**, 187 (1993).

[4] T. Sjostrand, S. Mrenna and P. Skands, JHEP **0605**, 026 (2006).

[5] T. Affolder *et al.* (CDF Collaboration), Phys. Rev. D **65**, 092002 (2002).

[6] D. Acosta *et al.* (CDF Collaboration), Phys. Rev. D **71**, 112002 (2005).

[7] *F. Abe et al.* [CDF Collaboration], Nucl. Instrum. Meth. **A271**, 387-403 (1988).

[8] *F. Abe et al.* [CDF Collaboration], The CDF-II detector: Technical design report, FERMILAB-PUB-96-390-E (1996).

[9] In the CDF and DØ coordinate system, ϕ is the azimuthal angle and θ is the polar angle with respect to the proton beam direction. The pseudo-rapidity η is defined as $\eta = -\ln\tan(\theta/2)$. The transverse momentum of a particle is $p_{\mathrm{T}} = p\sin\theta$. If the magnitude of this vector is obtained using the calorimeter energy rather than the spectrometer momentum, it becomes the transverse energy E_{T}. Jets are defined as clusters of energy in $\eta - \phi$ space with a fix cone size. The missing transverse energy ($\not\!\!E_{\mathrm{T}}$) is defined as the difference between the vector sum of all the transverse energies and zero.